Preparation of Porous TiO_2 Cryogel Fibers through Unidirectional Freezing of Hydrogel Followed by Freeze-Drying

Shin R. Mukai,* Hirotomo Nishihara, Seiji Shichi, and Hajime Tamon

Department of Chemical Engineering, Kyoto University, Katsura, Nishikyo-ku, Kyoto 615-8510, Japan

Received May 31, 2004. Revised Manuscript Received September 5, 2004

Porous titania cryogel fibers (TCFs) were prepared through the unidirectional freezing and subsequent freeze-drying of titania hydrogels, which were synthesized by sol−gel polymerization of titanium tetraisopropoxide (TTIP) using dialysis. By adjusting the concentrations of TTIP, and using freeze-drying after replacing the water included in the titania hydrogel fibers with *tert*-butyl alcohol, mesoporous TCFs which maintained their unique fiber morphology were successfully prepared. The as-dried TCFs were transparent, contained anatase structure, and had BET surface areas over 400 m^2/g. Nitrogen adsorption−desorption measurements, powder X-ray diffractometry (XRD), scanning laser microscopy, and scanning electron microscopy (SEM) were used to characterize the physical properties of TCFs. The effect of heat treatment after freeze-drying on the porous properties and crystal structures of TCFs was examined. It was found that BET surface areas and mesopore volumes of TCFs decrease with the increase in heat treatment temperature. On the other hand, the XRD peak intensity corresponding to anatase structure increases with the increase in heat treatment temperature in the range below 773 K. Photocatalytic decomposition activities of large organic molecules on TCFs was also measured and the results were compared with those from a commercial photocatalyst, Degussa P-25. Moreover, photocatalytic decomposition of methylene blue was examined by using TCF-packed columns.

Introduction

Titania (TiO_2) is known to be a photocatalyst, and has been used in various applications.[1−5] The mechanism of photocatalytic reactions is much different from that of typical catalytic reactions.[6] When the photocatalysts are irradiated by UV rays, highly reactive radical species (e.g., OH· and $\cdot O_2^-$) are generated from species adsorbed on the surface of photocatalysts such as water and oxygen. Such reactive species decompose organic compounds, or in some cases even inorganic compounds, which coexist on the surface of the photocatalysts. It is well-known that there are two typical crystal structures in titania: anatase and rutile. Anatase shows a higher photocatalytic activity than rutile, as its band gap energy is lower. Therefore, for efficient photocatalytic decomposition, the catalyst titania needs to have not only proper nanostructures which lead to high surface areas and high contents of anatase, but also a proper morphology, which can realize efficient mass-flow of reactants and irradiation of UV rays. Various attempts to control the morphology of titania have been made. Besides conventional morphology such as colloidal particles and thin films, various kinds of new morphology such as thin flakes,[7] hollow spheres,[8,9] nanotubes,[10,11] and microtubes[12] have been prepared. In this work, we describe the preparation of titania fibers with high surface areas, large mesopore volumes, and high contents of anatase.

Photocatalysts with fiber morphology have recently attracted great attention from their low pressure drops, short diffusion lengths, and superior transport abilities of light. They are usually prepared through the impregnation method, which essentially supports titania particles on fibrous materials such as optic cables,[13−15] glass

* To whom correspondence should be addressed. E-mail: mukai@cheme.kyoto-u.ac.jp

(1) Wold, A. *Chem. Mater.* **1993**, *5*, 280.
(2) Hoffmann, M. R.; Martin, S. T.; Choi, W. Y.; Bahnemann, D. W. *Chem. Rev.* **1995**, *95*, 69.
(3) Mills, A.; LeHunte, S. *J. Photochem. Photobiol. A* **1997**, *108*, 1.
(4) Wang, R.; Hashimoto, K.; Fujishima, A.; Chikuni, M.; Kojima, E.; Kitamura, A.; Shimohigoshi, M.; Watanabe, T. *Nature* **1997**, *388*, 431.
(5) Gratzel, M. *Nature* **2001**, *414*, 338.
(6) Linsebigler, A. L.; Lu, G. Q.; Yates, J. T. *Chem. Rev.* **1995**, *95*, 735.
(7) Sasaki, T.; Nakano, S.; Yamauchi, S.; Watanabe, M. *Chem. Mater.* **1997**, *9*, 602.
(8) (a) Iida, M.; Sasaki, T.; Watanabe, M. *Chem. Mater.* **1998**, *10*, 3780. (b) Wang, L.; Sasaki, T.; Ebina, Y.; Kurashima, K.; Watanabe, M. *Chem. Mater.* **2002**, *14*, 4827.
(9) Caruso, R. A.; Susha, A.; Caruso, F. *Chem. Mater.* **2001**, *13*, 400.
(10) (a) Hoyer, P. *Langmuir* **1996**, *12*, 1411. (b) Hoyer, P. *Adv. Mater.* **1996**, *8*, 857.
(11) (a) Kasuga, T.; Hiramatsu, M.; Hoson, A.; Sekino, T.; Niihara, K. *Langmuir* **1998**, *14*, 3160. (b) Kasuga, T.; Hiramatsu, M.; Hoson, A.; Sekino, T.; Niihara, K. *Adv. Mater.* **1999**, *11*, 1307.
(12) Peng, T. Y.; Hasegawa, A.; Qiu, J. R.; Hirao, K. *Chem. Mater.* **2003**, *15*, 2011.
(13) Hofstadler, K.; Bauer, R.; Novalic, S.; Heisler, G. *Environ. Sci. Technol.* **1994**, *28*, 670.
(14) Peill, N. J.; Hoffmann, M. R. *Environ. Sci. Technol.* **1995**, *29*, 2974.
(15) Rice, C. V.; Raftery, D. *Chem. Commun.* **1999**, *10*, 895.

10.1021/cm0491328 CCC: $27.50
Published on Web 11/03/2004

fibers,[16,17] activated carbon fibers,[18,19] cellulose fibers,[20] etc. However, supported catalysts are likely to be degraded through sintering, attrition, etc.[21] Therefore, it is preferable to prepare self-constructed titania fibers with high surface areas and high contents of anatase. Several methods have been presented for the preparation of such titania fibers. Kamiya et al.[22] have prepared self-constructed titania fibers by drawing viscous titania sols, and Yin et al.[23] have prepared titania short fibers by the heat treatment of $H_2Ti_4O_9{\cdot}nH_2O$. Besides these direct-synthesis methods, two-step synthesis methods, which use organic fibers as templates[24,25] or composites of titania−polymer as precursors,[26] have been reported. Although it is possible to prepare titania fibers with well-organized structures by using such methods, the BET surface areas of the obtained titania fibers are extremely low, normally less than 100 m^2/g.

Titania aerogels, which are prepared by sol−gel polymerization followed by subsequent supercritical drying, have both high surface areas and high contents of anatase.[27,28] It has been shown that titania aerogels have a high photocatalytic ability to decompose organic pollutants in aqueous environments,[29] including NO,[30] benzene,[31] phenol para-derivatives,[32] etc. In this work, we attempted to synthesize self-constructed titania fibers with high surface areas and large mesopore volumes such as aerogels. However, the cost of supercritical drying is expensive as it requires special equipment and long drying time. Therefore, we used a more economical drying method, freeze-drying,[33,34] to synthesize porous titania cryogels with high contents of anatase. As for the preparation method of titania fibers, we adopted the unidirectional freezing method,[35] which uses polygonal ice rods as templates and can be combined with subsequent freeze-drying processes. Unidirectional freezing is a kind of ice-templating method,[36,37] which does not need template-additives and subsequent processes to remove them, such as calcination and chemical treatment. In the ice-templating method, ice crystals, which are grown in situ and can be easily removed by thawing followed by drying, act as the template, therefore porous materials with high purity can be easily prepared. Hence, this method can be said to be a low-cost and environmentally friendly method to prepare functional materials. Here we describe the preparation of porous titania cryogel fibers (TCFs) using unidirectional freezing of titania hydrogel followed by freeze-drying. The porous properties, crystal structure, and photocatalytic properties of the prepared TCFs are also reported in detail.

Experimental Section

Preparation of TCFs. TiO_2 hydrogels were synthesized by the polymerization of TTIP in an ethanol/water mixture using HCl as the catalyst, followed by dialysis. The molar ratio among TTIP/water/HCl was fixed to 1:1.9:0.53, and the molar ratio of ethanol/TTIP (this ratio will be denoted as Et/Ti, hereafter) was varied. First, a TTIP solution was prepared by dissolving TTIP (Wako Chemical, Inc., research grade) in ethanol, the amount of which was adjusted to be half of the designated total amount, at room temperature. Next, a HCl solution was prepared by mixing an aqueous solution of HCl (Wako Chemical, Inc., research grade, 36 wt % HCl dissolved in water) in the remaining portion of ethanol. Then the HCl solution was added very slowly to the ice-cooled and vigorously stirred TTIP solution. The resulting clear solution was poured into a tube of cellulose dialysis membrane (Spectrum Laboratories, Inc., MWCO = 3500, diameter = 11.5 mm). Dialysis was carried out by immersing the dialysis tube into 2 L of distilled and deionized water, which was refreshed every 24 h. This period of dialysis will be denoted as t_{dia}, hereafter. After dialysis, a transparent TiO_2 hydrogel was formed inside the dialysis tube. Then the tube was placed into a glass cylinder (diameter 25 mm), which was filled with distilled and deionized water, and the cylinder was unidirectionally frozen by immersing it perpendicularly into a cold bath of liquid nitrogen at a constant rate of 6 cm/h. After the whole sample was frozen and fiber structures were constructed, the cylinder was moved to another cold bath maintained at 243 K, and was aged in it for 24 h in order to strengthen the fiber structures under a condition where ice crystals serve as templates. Then the frozen sample was quickly thawed at 327 K.

The thawed titania hydrogel fibers were filled with water, which is likely to destroy the fiber structure and porous structure at the freeze-drying stage. Therefore, titania hydrogel fibers were thoroughly washed with *tert*-butyl alcohol before freeze-drying.[36,37] After the water contained in the titania hydrogel fibers was replaced by *tert*-butyl alcohol, they were freeze-dried at 263 K for 3 days and TCFs were obtained. Some TCFs were calcinated for 2 h at temperatures set in the range of 573 to 1023 K.

Characterization. The micromorphology and nanostructures of TCFs were directly observed using a laser scanning confocal microscope (Keyence Japan Inc.; VK-8550) and a scanning electron microscope (SEM, JEOL Japan Inc.; JSM-6340FS). Porous properties of TCFs were analyzed from nitrogen adsorption−desorption isotherms obtained at 77 K; BET surface areas, S_{BET}, were calculated through the Brunauer−Emmett−Teller (BET) method; and mesopore size distributions and mesopore volumes, V_{mes}, were calculated through the Dollimore−Heal method applied to the desorption isotherms. Note that the range of mesopore size used in the calculation of V_{mes} is 2−50 nm in diameter, as defined by IUPAC. The crystal structures of TCFs were investigated using

(16) Pichat, P.; Disdier, J.; Hoang-Van, C.; Mas, D.; Goutailler, G.; Gaysse, C. *Catal. Today.* **2000**, *63*, 363.
(17) Horikoshi, S.; Watanabe, N.; Onishi, H.; Hidaka, H.; Serpone, N. *Appl. Catal. B* **2002**, *37*, 117.
(18) Reztsova, T.; Chang, C. H.; Koresh, J.; Idriss, H. *J. Catal.* **1999**, *185*, 223.
(19) Yamashita, H.; Harada, M.; Tanii, A.; Honda, M.; Takeuchi, M.; Ichihashi, Y.; Anpo, M.; Iwamoto, N.; Itoh, N.; Hirao, T. *Catal. Today* **2000**, *63*, 63.
(20) Goutailler, G.; Guillard, C.; Daniele, S.; Hubert-Pfalzgraf, L. G. *J. Mater. Chem.* **2003**, *13*, 342.
(21) Bartholomew, C. H. *Appl. Catal. A* **2001**, *212*, 17.
(22) Kamiya, K.; Tanimono, K.; Yoko, T. *J. Mater. Sci. Lett.* **1986**, *5*, 402.
(23) Yin, S.; Sato, T. *Ind. Eng. Chem. Res.* **2000**, *39*, 4526.
(24) Imai, H.; Matsuta, M.; Shimizu, K.; Hirashima, H.; Negishi, N. *J. Mater. Chem.* **2000**, *10*, 2005.
(25) Hozumi, A.; Itoh, T.; Yokogawa, Y.; Kameyama, T. *J. Mater. Sci. Lett.* **2002**, *21*, 897.
(26) Fan, C. L.; Ciardullo, D.; Huebner, W. *J. Mater. Res.* **2003**, *18*, 687.
(27) Campbell, L. K.; Na, B. K.; Ko, E. I. *Chem. Mater.* **1992**, *4*, 1329.
(28) Suh, D. J.; Park, T. J. *Chem. Mater.* **1996**, *8*, 509.
(29) Dagan, G.; Tomkiewicz, M. *J. Phys. Chem.* **1993**, *97*, 12651.
(30) Reiche, M. A.; Ortelli, E.; Baiker, A. *Appl. Catal. B* **1999**, *23*, 187.
(31) Yoda, S.; Suh, D. J.; Sato, T. *J. Sol−Gel Sci. Technol.* **2001**, *22*, 75.
(32) Malinowska, B.; Walendziewski, J.; Robert, D.; Weber, J. V.; Stolarski, M. *Appl. Catal. B* **2003**, *46*, 441.
(33) Tamon, H.; Ishizaka, H.; Yamamoto, T. Suzuki, T. *Carbon* **1999**, *37*, 2049.
(34) Mukai, S. R.; Nishihara, H.; Tamon, H. *Microporous Mesoporous Mater.* **2003**, *63*, 43.
(35) Maki, T.; Teranishi, Y.; Kokubo, T.; Sakka, S. *Yogho-kyokai-shi* **1985**, *93*, 387.
(36) Mukai, S. R.; Nishihara, H.; Tamon, H. *Chem. Commun.* **2004**, *7*, 847.
(37) Nishihara, H.; Mukai, S. R.; Tamon, H. *Carbon* **2004**, *42*, 899.

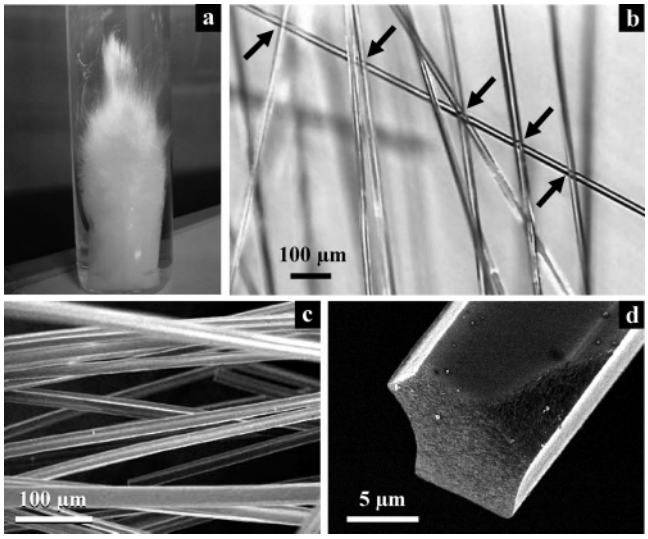

Figure 1. Images of typical TCFs (Et/Ti = 1.0 and t_{dia} = 48 h): (a) overall image; (b) laser scanning confocal microscope image. SEM images of (c) bundle of TCFs and (d) cross-section of a TCF.

a powder X-ray diffractometer (XRD, Rigaku Co. Ltd.; RINT2100) with Cu Kα radiation under the power of 40 kV and 40 mA.

Photocatalytic Properties. To compare the photocatalytic properties of TCFs directly with that of a commercial photocatalyst, Degussa P-25, TCFs were powdered and their photocatalytic abilities to decompose salad oil (Nisshin salad oil, Nisshin Oillio Group, Ltd.) were compared. Salad oil contains large molecules such as oleic, linoleic, linolenic, palmitic, and stearic acids, and is thought to be a good reactant to test photocatalysts for self-cleaning applications.[38] Powdered samples (ca. 0.17 g) were mixed with salad oil at a weight ratio of 6:1, and the resulting slurries were evenly coated on the bottom of plastic cells (length 68 mm, width 39 mm, height 15 mm). The cells were placed in a dark vessel (temperature 298 K, relative humidity 25%). Then the cells were irradiated with UV rays (1 mW/cm^2) emitted from a black light lamp (AS ONE Inc.; LUV-6, 6 W) and the changes in their weights were measured.

To investigate the advantages of the fiber morphology of TCFs, photocatalytic decomposition of methylene blue was carried out using a column packed with TCFs. A bundle of TCFs was immersed into a methylene blue solution. After sufficient time had passed so that the adsorption of methylene blue reached equilibrium, the immersed sample was air-dried and packed into a glass column (inner diameter 4 mm, length 30 mm). Then the column was illuminated with UV rays from only one side under the same conditions using the same apparatus described above, and the change in its color was observed.

Results and Discussion

Micromorphology and Nanostructure of TCFs. An overall image of a typical as-dried TCF is shown in Figure 1a. A bundle of self-constructed long TCFs wrapped by a dialysis tube can be seen inside the glass cylinder, which was used during unidirectional freezing, solvent replacement, and freeze-drying. In unidirectional freezing, template ice rods grow in situ in parallel with the freezing direction. Therefore, a bundle of unidirectionally aligned fibers is obtained after the removal of the template ice rods by thawing and drying.

(38) Minabe, T.; Tryk, D. A.; Sawunyama, P.; Kikuchi, Y.; Hashimoto, K.; Fujishima, A. *J. Photochem. Photobiol. A* **2000**, *137*, 53.

Table 1. Preparation Conditions and Physical Data of As-Dried TCFs

sample	Et/Ti[a]	t_{dia}[b] (h)	shape	S_{BET}[c]	V_{mes}[d] (cm^3/g)	d_{peak}[e] (nm)
TCF-1	3.0	6	powder	nm[f]	nm	nm
TCF-2	1.0	24	fiber	510	0.25	2.1
TCF-3	1.0	48	fiber	378	0.49	3.8
TCF-4	3.0	48	fiber	430	0.53	3.5
TCF-5	3.0	54	fiber	334	0.54	5.1
TCF-6	5.0	144	fiber	291	0.32	3.7

[a] Molar ratio of ethanol/titanium tetraisopropoxide. [b] Dialysis time. [c] BET specific surface area. [d] Mesopore volume calculated from Dollimore−Heal method applied to desorption isotherms. [e] Peak diameters of mesopore size distributions. [f] nm: Not measured.

Figure 1b shows a laser scanning micrograph of TCFs. The diameters of TCFs were in the range of 10−30 μm, and their lengths were several centimeters. Therefore, it can be said that the TCFs have the same morphology as commercial glass fibers, which are popularly used as the supports for the preparation of titania/silica fiber photocatalysts. Moreover, it was confirmed that TCFs prepared in this work are transparent, as can be seen in the regions pointed out by arrows in Figure 1b. This indicates that TCFs are composed of nanoparticles whose diameters are less than the wavelength of visible light. To confirm this, SEM observation was carried out. The SEM images of the TCFs and the cross-section of a TCF are shown in Figure 1c and d, respectively. In Figure 1d, it can be seen that TCFs have polygonal cross-sections and their outside surfaces look smooth. On the other hand, it can be seen that the inside of a TCF is composed of extremely small nanoparticles. Such a system is same as cryogels of other materials.[36,39] Therefore, the spaces between the nanoparticles can be thought to be the origin of the mesoporosity of TCFs.

Effects of Synthesis Conditions. The effects of Et/Ti and t_{dia} on the shape and porous properties of TCFs are summarized in Table 1. It was found that TCFs can be prepared in a wide range of Et/Ti, and Et/Ti hardly affects the shape and porous properties of TCFs. However, long TCFs could not be obtained when Et/Ti was smaller than 1.0. On the other hand, the duration of dialysis, t_{dia}, was found to affect both the shape and porous properties of TCFs. When t_{dia} was less than 24 h as for TCF-1, only powder, which is aggregations of extremely short fibers could be obtained. This is because the polymerization of titania gels had not been fully completed, so the resulting TCFs were fragile. Long TCFs could be prepared when t_{dia} was longer than 24 h. The effect of t_{dia} on the porous properties of TCFs is compared in Figure 2 and Figure 3. Both V_{mes} and d_{peak} increased with the increase in t_{dia} in the range below 54 h. This is thought to be the result of Ostwald ripening, through which micropores decrease and mesopores increase. From Figure 3, it can be seen that TCF-3 and TCF-5 have developed mesopores, which are thought to be suitable for the photocatalytic decomposition of large molecules. However, an excessive t_{dia} resulted in the decrease in mesoporosity and S_{BET}, as can be confirmed from the data of TCF-6 in Table 1. This is thought to be the consequences of the syneresis of titania hydrogels accompanied by significant shrinkage. It is known that when excessive aging is conducted syneresis of titania hydrogels becomes extreme, and

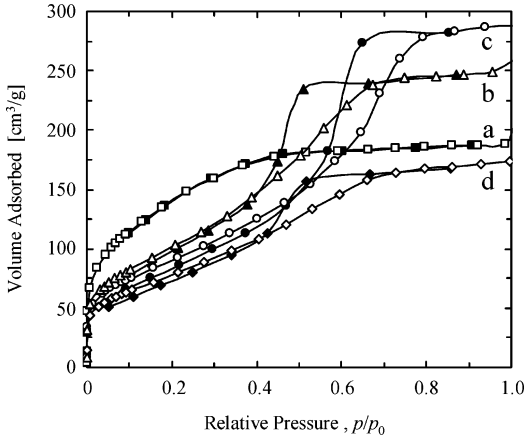

Figure 2. Adsorption−desorption isotherms of N_2 on as-dried TCFs prepared by different t_{dia}: (a) TCF-2, (b) TCF-3, (c) TCF-5, and (d) TCF-6.

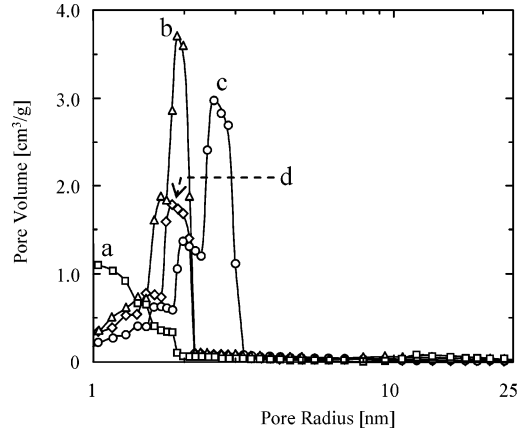

Figure 3. Mesopore size distributions of as-dried TCFs prepared by different t_{dia}: (a) TCF-2, (b) TCF-3, (c) TCF-5, and (d) TCF-6.

they are likely to shrink.[40] In fact, a significant shrinkage of titania hydrogel was observed in TCF-6. Therefore, it can be concluded that t_{dia} should be in the range around 48 h.

Effects of Heat Treatment. Figure 4 shows the change in the XRD pattern induced by heat treatment at various temperatures, along with the XRD pattern of P-25. It was found that TCFs contain anatase structure even at the as-dried stage. The intensity of the peak corresponding to anatase structure increased with the increase in the heat treatment temperature in the range below 773 K. Rutile structure was found to develop at temperatures above 873 K. On the other hand, both S_{BET} and V_{mes} decreased with the increase in the heat treatment temperature as shown in Figure 5. These results of TCFs, titania cryogels, are consistent with the results of titania aerogels.[27] It can be said that the porous properties of both titania cryogels and titania aerogels are likely to be deteriorated by heat treatment. However, considering their usage as photocatalysts, heat-treatment before usage is not always necessary. Therefore, considering their high porosity and high anatase contents, TCFs heat-treated at temperatures

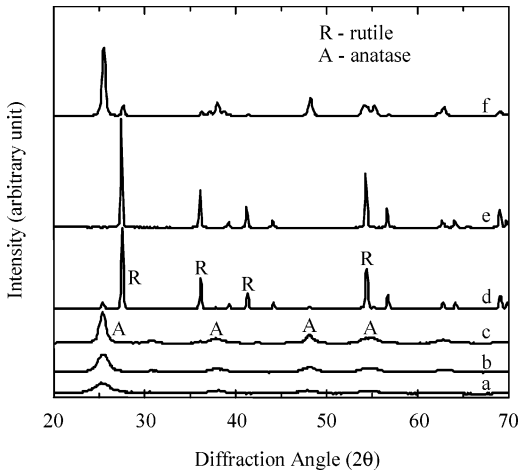

Figure 4. Effect of heat treatment on the crystal structure of TCFs as determined by X-ray diffractometry: (a) as-dried TCF-4; TCF-4 heat treated at (b) 673 K, (c) 773 K, (d) 873 K, and (e) 1023 K; and (f) commercial photocatalyst, P-25.

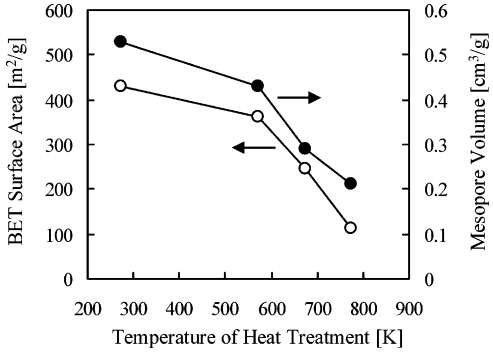

Figure 5. Effect of heat treatment on the BET surface area and mesopore volume of TCFs.

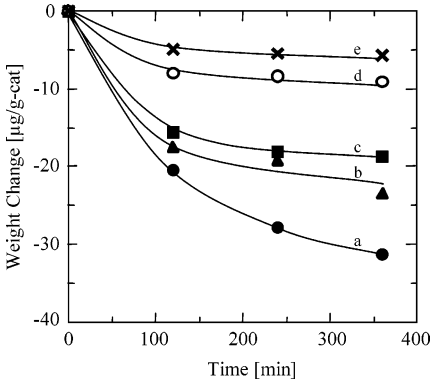

Figure 6. Weight change against the illumination time in the photocatalytic decomposition of salad oil: (a) as-dried TCF-4; TCF-4 heat treated at (b) 573 K, (c) 673 K, and (d) 773 K; and (e) commercial photocatalyst, P-25.

under 773 K are expected to show high photocatalytic activities.

Photocatalytic Properties of TCFs. Figure 6 compares the photocatalytic activities of P-25 and TCFs. It was found that all of the TCFs synthesized in this work had higher photocatalytic decomposition abilities toward salad oil, a model reactant representing large-molecular organic substances. Such superior activities of TCFs are thought to come from their higher BET surface areas and larger mesopore volumes (the S_{BET} and V_{mes} of P-25 were 45 m^2/g and 0.09 cm^3/g, respectively). Moreover, the order of differences in the photocatalytic reactivities

(39) Yamamoto, T.; Nishimura, T.; Suzuki, T.; Tamon, H. *J. Non-Cryst. Solids* **2001**, *288*, 46.
(40) Brinker, C. J.; Scherer, G. W. *Sol−Gel Science*; Academic Press: Boston, MA, 1990.

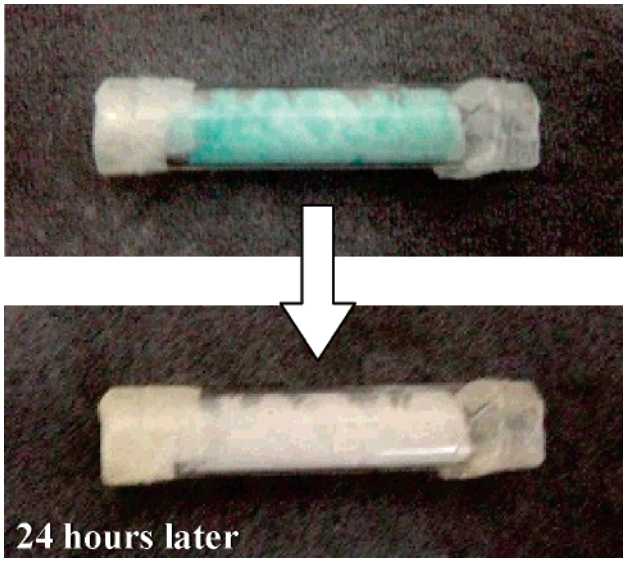

Figure 7. Images of the TCF-packed columns before (upper) and after (lower) the photocatalytic decomposition of methylene blue.

matches the order of differences in their S_{BET} and V_{mes} values. Therefore, it can be concluded that improving the porous properties of photocatalysts is very effective to enhance their photocatalytic decomposition activities, in cases where large-molecular substances are involved.

Finally, we examined the advantages of the fiber morphology of TCFs. Figure 7 shows the methylene blue equilibrated TCFs prior to and after irradiation of UV rays. At 24 h after the start of irradiation of UV rays, the blue color of the fibers had completely vanished even in the dark side of the column. Methylene blue is known to be a good test reactant for the characterization of photocatalytic activities because they do not react under UV rays without photocatalysts. Therefore, all of the methylene blue inside the column must have been degraded through photocatalytic decomposition, even that in the dark side of the column. This result strongly indicates that the UV rays had reached the dark side of the column. Therefore, it can be said that TCF-packed columns show high activities in photocatalytic reactions from their high transport abilities of UV rays, excellent porosity, and high content of anatase structure.

Conclusions

Porous titania cryogels with anatase structure were successfully tailored into long and thin fibers by using unidirectional freezing for the formation of fiber morphology and freeze-drying for the development of porosity. Conventional procedures for the preparation of titania fibers often include heat treatment or high-temperature calcination processes (523−1073 K) which usually leads to the decrease in surface area and pore volume.[23−26] In our proposed procedure, ice crystals grown in situ mold porous titania gels into a fiber shape, and a poreprotecting method, freeze-drying, is adopted to dry the molded fibers. Moreover, this procedure does not require heat treatment or calcination. These are thought to be the reasons why TCFs have higher BET surface areas and larger mesopore volumes when compared with those of conventional titania fibers. It was confirmed that TCFs show higher photocatalytic activities toward the decomposition of large organic molecules than a commercial photocatalyst, P-25. Moreover, when packed in a column, they showed good transport abilities of UV rays. The TCFs prepared in this work are expected to be used for various purposes as a highly efficient photocatalyst.

Acknowledgment. This research was partially supported by the Japan Society for the Promotion of Science, Grant-in Aid for Scientific Research (B) 16360383 (2004), and Grant-in Aid for Young Scientists (B) 15760569 (2004).

CM0491328